Computer-Aided Diagnosis of Abdominal Aortic Aneurysms

Barry J. Doyle and Timothy M. McGloughlin

Abstract Computer-aided diagnosis (CAD) systems have been used in several areas of medicine for the last number of years. A typical CAD system interprets medical images and provides guidance for the clinician. The concept of CAD in the assessment of abdominal aortic aneurysm (AAA) has been around for several years, however, the technique is gaining momentum as of late. Computer modeling of AAAs is becoming more prevalent with several novel approaches of CAD reported over the past number of years. CAD is possible through computer-aided detection (CADe) and computer-aided quantification (CADq) techniques that work together to return usable quantities aimed at helping identify AAAs that may be at risk of rupture. This chapter examines some recent developments within the area of CAD for AAAs, in particular the use of peak wall stress, and also asymmetry and the finite element analysis rupture index. All three tools provide additional data to the clinician through the CAD system and help complement the use of maximum diameter in identifying high-risk AAAs.

1 Background

Abdominal aortic aneurysms (AAAs) are notoriously asymptomatic and often referred to as a "silent killer". Patients frequently present at hospital with abdominal and/or back pain, where examination reveals the cause of the pain to be

B. J. Doyle (✉) · T. M. McGloughlin
Department of Mechanical, Aeronautical and Biomedical Engineering, Materials and Surface Science Institute, Centre for Applied Biomedical Engineering Research (CABER), University of Limerick, MSSI Building, MSG-013-022, Limerick, Ireland
e-mail: Barry.Doyle@ul.ie

Stud Mechanobiol Tissue Eng Biomater (2011) 7: 119–138
DOI: 10.1007/8415_2011_70

Published Online: 24 April 2011

a pulsating mass deep within the abdomen, in other words, an AAA. Ultrasound is the preferred method to diagnose AAAs, primarily because the tool is cost effective and measurements are reproducible within a range of 6 mm [16]. Screening involves the use of ultrasonography to detect AAA and the implementation of these programs is becoming increasingly common. It has been recommended that people over the age of 60–65 years, in particular men, should be screened for AAA, with the recommended age reducing to 50–55 when there is a history of aneurysmal disease in the family. AAA screening programs are becoming more widespread in the UK with many private institutions providing screening. The UK National Health Service (NHS) recently announced that a full screening program will be made available throughout the UK, but is unlikely to become widely available until 2013 [38]. According to the US Preventative Services Task Force [55], the potential benefit of screening for AAA among women over the age of 65 is low because of the number of age-related deaths in this population. The majority of AAA related deaths occur in women over the age of 80, and as there are many competing health risks at this age, any benefit of screening would be minimal [55].

Currently, the trend in determining the severity of an AAA is to use the maximum diameter criterion [4, 22]. Patients with an AAA that has a maximum diameter greater than 5–5.5 cm are deemed a high rupture risk and are usually recommended for surgical repair [26]. In the case of smaller AAAs where the diameter <5 cm, the preferred approach is often careful and frequent observation using either ultrasonography or computed tomography (CT). AAA growth rate is also used as an additional parameter with AAAs that exceed growth rates of 1 cm/year deemed a high rupture risk. Recent research however, has questioned the suitability of surgical repair based on the maximum diameter criterion alone [9, 10, 13, 18, 19, 25, 27, 41, 46, 57–59]. Although the diameter-criterion can be justified, as the rupture risk for an AAA is clearly related to its maximum diameter [3, 18], surgical decision-making using solely this parameter may in fact lead to unnecessary AAA repairs and also exclude certain cases (AAA < 5 cm) from surgical repair [4, 5, 18, 40]. Nicholls et al. [40] reported that 10–24% of ruptured AAAs were less than 5 cm in diameter. Darling et al. [5] also reported that of 473 non-repaired AAAs examined from autopsy reports, there were 118 cases of rupture, 13% of which were less than 5 cm in diameter. They also showed that 60% of the AAAs greater than 5 cm (including 54% of those AAAs between 7.1 and 10 cm) never experienced rupture. Vorp et al. [62] later concluded from the findings of Darling et al. [5] that if the maximum diameter criterion were followed for the 473 subjects, only 7% (34/473) of cases would have succumbed to rupture prior to surgical intervention as the diameter was less than 5 cm, with 25% (116/473) of cases possibly undergoing unnecessary surgery since these AAAs may never have ruptured.

Alternative approaches to rupture assessment have been recently reported. The majority of these methods involve the numerical analysis of AAAs using the common engineering technique of the finite element method (FEM) to determine the wall stress distributions. Studies have reported that these stress distributions

correlate to the overall geometry of the AAA rather than to the maximum diameter [9, 45, 63]. It is also known that wall stress alone does not completely dictate failure as an AAA will rupture when the local wall stress exceeds the local wall strength. Therefore, rupture risk should consider the patient-specific wall stress along with the patient-specific wall strength. A non-invasive method of approximating patient-specific wall strength was recently reported by Vande Geest et al. [57–59], with more traditional approaches to strength determination via tensile testing performed by others [6, 42, 44, 52, 68]. Newly proposed AAA rupture risk parameters include: AAA wall stress [18, 19, 60]; AAA expansion rate [23]; degree of asymmetry [9]; presence of intraluminal thrombus (ILT)[1] [65]; a rupture potential index (RPI) [57, 58]; a finite element analysis rupture index (FEARI) [10, 13]; biomechanical factors coupled with computer analysis [25]; growth of ILT [50]; geometrical parameters of the AAA [9, 21]; and also a method of determining AAA growth and rupture based on mathematical models [61, 66]. Based on this recent work by both our group and others, it is believed that improved AAA rupture risk parameters are necessary and could have major clinical relevance.

As computational modeling, and computers in general, become a vital tool for clinicians in all aspects of healthcare, the role of CAD systems will become more prevalent. This chapter will briefly describe the use of CAD for AAAs and also present the preliminary validation of computational modeling for AAA rupture-prediction.

2 Computer-Aided Diagnosis (CAD)

Computer modeling has become an important tool in the clinical work flow when treating several types of disorders as there is significant potential to improve diagnosis, optimise clinical treatment by predicting outcomes, and inform the design of surgical training practices [39]. This approach is becoming more prevalent in AAA treatment nowadays [11] as clinicians become more aware of the ease in which patient-specific modeling can be applied to the disease. CAD can be applied to AAAs to identify those aneurysms that are a high rupture risk, and also indicate AAAs that may be relatively safe from rupture, thus preventing the trauma and cost associated with surgical treatment. CAD can be divided into a sequence of Computer-Aided Detection (CADe) and Computer-Aided Quantification (CADq), whereby CADe entails the detection, medical imaging and three-dimensional (3D) reconstruction of the model, and CADq encompasses some of the recently proposed parameters that aim to improve the determination of rupture risk. These terms have been adapted from their regular use in radiology, in particular, the use of CAD systems in mammography [17], to suit the current application of AAAs.

[1] ILT consists of a fibrin structure incorporated with blood cells, platelets, blood proteins and cellular debris, and are found in most AAAs.

The impact computers have had on medical imaging over recent years is indisputable, as without computers, imaging modalities such as CT or magnetic resonance imaging (MRI) would not even exist. However, the interpretation of medical images is still a human task and this is set to continue for many years as false positives are hard to rule out when relying on computers alone. There is immense research, in particular within the area of cancer research, to help reduce false positive readings and allow image interpretation to become an automated process. Whilst it is unlikely that AAA diagnosis will ever become completely automated, the role of computers must not be under-estimated. CADe systems will allow the AAA to be properly detected and reconstructed, whereas CADq systems allow an estimate of rupture risk to be determined. This process is semi-automated and requires significant user input, with some attempting to almost remove the user input by designing software to perform the CADe and CADq elements (A4 Clinics™, VASCOPS GmbH, Austria). The use of finite element analysis (FEA) to predict rupture locations in AAAs has recently been validated in vitro [12, 14] with some preliminary results of in vivo validation described later on in this chapter.

3 Computer-Aided Detection (CADe)

When concerned with AAAs, CADe refers to the imaging of the aneurysm and the subsequent 3D reconstruction. Initial examination of a patient suspected of AAA is usually performed via ultrasound. Ultrasound can identify AAAs and allow maximum diameter measurements, however, if any further examination of the disease is required, CT, or in some cases MRI, must be employed. CT capabilities vary from institution to institution, with the performance potential of CAD systems heavily dependent on the initial image quality. Poor pixel resolution of the scans will result in poor image interpretation, poor reconstructions and ultimately, poor diagnosis. For the purposes of this chapter, CADe will entail the use of the commercially available software Mimics (Materialise NV, Belgium) which has been used in several reports in the literature [7–11, 13, 30, 31, 67]. The process of reconstruction using Mimics has been reported in-depth previously [8] but in essence relies on thresholding and segmentation of the CT image. Thresholding is based on the pixel intensity, often measured in Hounsfield Units (HU), and allows the user to identify regions of interest, in this case the AAA. Segmenting the AAA from the remainder of the image is then possible and can be applied to every scan in the series. Mimics employs the *marching cubes* and *marching squares* algorithms [29] to produce a triangle mesh by computing isosurfaces from discrete data. From connecting the patches from all the cubes on the isosurface boundary, a surface representation can be obtained. This procedure, as shown in Fig. 1, results in 3D models of exquisite detail, which can be further refined and smoothed by the user if desired.

The majority of AAAs contain intraluminal thrombus. In computational models, this thrombus has been shown to significantly alter the biomechanics of the

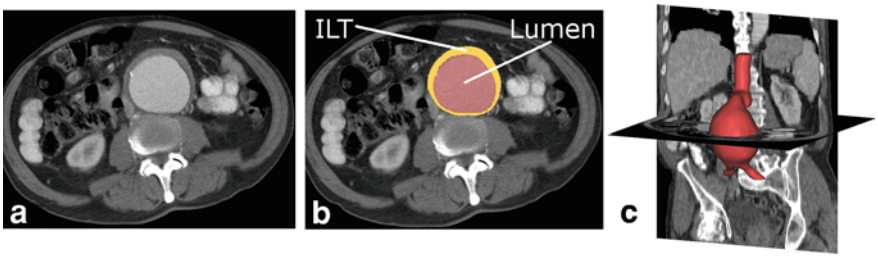

Fig. 1 Procedure of 3D reconstruction from CT scan. **a** Typical CT scan of an AAA through the maximum diameter region. **b** Image after thresholding and segmentation of the region of interest with the lumen shown in *yellow* and the intraluminal thrombus (ILT) shown in *blue*. **c** Resulting 3D reconstruction of the AAA

aneurysm, yet, it has been reported that in vivo pressure transmission through the thrombus can vary considerably from patient to patient [56] and may not act as the "mechanical buffer" that it is often described as. Regardless of the on-going debate over the role of the ILT, from both clinical [47] and engineering [1] viewpoints, the structure must be included in numerical models if rupture-prediction estimates are desired. In 2001, Wang and colleagues [64] mechanically characterised the ILT using 50 specimens harvested from 14 patients. The resulting population-mean material model is possibly the most employed throughout the literature and is applied to all FEA computations in this chapter.

Calcifications are also a common feature of AAAs. Calcified deposits primarily occur within the intima and intima-media interface, but can also occur within the ILT. The role of calcifications in numerical analyses is still somewhat under debate and is strongly dependent on the modeling approach. Speelman et al. [49] modeled calcifications by assigning modified material properties to regions of the diseased AAA wall, whereas Li et al. [28] included the structures as separate entities. More recently, Maier et al. [31] examined several different approaches to calcification inclusion and concluded that it is doubtful that rupture risk will increase by including calcified deposits in numerical models as they can act as load bearing structures. Inclusion of calcifications are therefore omitted from the CAD aspects of this chapter, but could be easily implemented in future studies should the role of these deposits be clarified.

The cohort included for examination in this present study consists of both electively-repaired ($n = 42$) and ruptured ($n = 10$) AAA cases, of which the general details and AAA characteristics are shown in Table 1.

4 Computer-Aided Quantification (CADq)

Computer-Aided Quantification (CADq) can take several forms in the context of AAA assessment. The current clinical standard used to quantify AAA rupture-threat is to measure the maximum diameter and, if possible the growth rate, of the

Table 1 Patient details and AAA characteristics of study cohort (Mean ± SD)

	Repaired	Ruptured	*P*
n	42	10	–
Male/female	34/8	7/3	–
Age	71.9 ± 6.4	69.1 ± 6.0	0.205
Diameter (mm)	64.3 ± 12.7	81.7 ± 12.5	0.0003
AAA volume (cm^3)	228.2 ± 119.6	428.8 ± 120.8	0.015
% ILT	50.9 ± 20.1	39.5 ± 14.8	0.057
Surface area (cm^2)	209.3 ± 73.7	317.1 ± 101.8	0.009
Length (mm)	111 ± 16	131 ± 25	0.03
Diameter/length	0.58 ± 0.09	0.63 ± 0.09	0.138
ROD[a]	2.05 ± 0.45	2.26 ± 0.53	0.268

[a] Ratio of maximum diameter to proximal neck diameter

aneurysm. However, as discussed earlier, there is growing concern over the use of these parameters in all AAA cases. Small AAAs can have similar, if not higher wall stress than much larger AAAs, and vice versa. Recent research suggests that more than size alone may contribute to rupture risk, however, reports [5] show that larger AAAs are more likely to rupture than smaller AAAs and therefore clinicians will seldom, if ever, recommend surveillance for large AAAs. Thus, biomechanical analysis of AAAs may only be applicable for small to medium-sized AAAs.

Over recent years, several laboratories have aimed at developing more robust rupture parameters than size alone. The Law of Laplace relates wall stress and diameter in a linear fashion and can estimate the wall stress exhibited on a cylinder. However, the Law fails to approximate the wall stress in more complex shapes and is therefore not suitable for AAAs. The use of computational techniques such as the finite element method (FEM) have allowed the wall stresses in these complex 3D AAA structures to be estimated and also provides an indication of the likely rupture location. For a detailed introduction and background into the FEM the reader can is referred to Zienkiewicz et al. [69]. Numerical results obtained using the FEM indicate the maximum wall stress in the model and usually generate a contour plot showing the distribution of wall stresses in the aneurysm. FEM uses the 3D geometry created from the medical images, converts the geometry into a series of elements connected with nodes, applies user-defined material properties and boundary conditions to the model, and then solves the problem to determine the stresses and strains within the structure. This process is illustrated in Fig. 2. For the purposes of the numerical analyses presented throughout this chapter the ILT was modeled using the material characteristics developed by Wang et al. [64] and the diseased AAA wall assigned the material model proposed by [41]. All analyses were performed using the commercially available finite element code ABAQUS v6.9 (SIMULIA, RI, USA). A static internal pressure of 120 mmHg (16 kPa) was applied to the luminal surface of all models and each AAA was rigidly constrained at the proximal and distal regions to represent the tethering to the remainder of the aorta. These are the standard boundary conditions used throughout the literature when analysing AAAs using

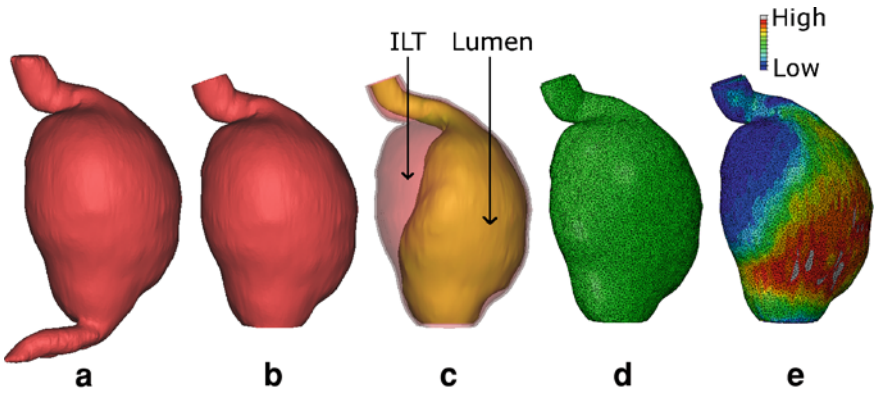

Fig. 2 **a** Complete 3D reconstruction of the AAA from above the mesenteric arteries to below the iliac bifurcation. **b** For the FE simulations, only the region from below the renal arteries to immediately above the iliac bifurcation is examined. **c** Each 3D reconstruction consists of the lumen region and the ILT. An artificial 1.5 mm uniform wall is then created around the ILT. **d** The 3D model is meshed and the appropriate boundary conditions applied. **e** Resulting von Mises stress contours on the model. In this particular case the large volume of ILT (86% of the total AAA volume) is shielding the diseased outer AAA wall from the force of the blood pressure resulting in very low wall stress in regions of thick ILT. All models are shown from the *right*

the FEM. Smoothing is necessary on 3D reconstructions of AAAs and the geometries used in the work presented here was smoothed according to a previous study [7] whereby all models are smoothed so that unwanted surface artefacts are removed without a significant loss in the accuracy of the structure. Other methods of smoothing have also been described [35, 36] and the process is currently very much user-dependent. There is no defined standard with respect to smoothing of AAAs and therefore care must be taken when generating reconstructions, with results analysed under several different levels of smoothing to assess the direct influence on 3D models.

CADq techniques using the FEM have allowed several novel approaches to AAA assessment to be proposed. Peak wall stress, the FEARI and asymmetry, and the severity parameter (SP) [25] have all been recently suggested as possible indicators of rupture risk. This chapter, however, will further describe the use of peak wall stress, FEARI and asymmetry within the context of AAA rupture-prediction.

4.1 Peak Wall Stress

Since the FEM was first applied to the problem of AAA in the late 1980's by Stringfellow et al. [51] the method has become the primary tool used to predict the stress exerted on the diseased AAA wall. In this first study [51] the aneurysm geometry was idealised as either 2D cylindrical or spherical. However, this work paved the way for others to investigate AAA disease using the FEM.

In the early 1990's, several others performed wall stress estimations using the FEM [15, 24, 37], again using idealised 2D geometries. These early studies were far from close approximations of the realistic wall stress experienced in vivo, yet they did introduce some important and still debatable topics that may influence wall stress. ILT was first included in numerical analyses by Inzoli et al. [24] in which they concluded that not only does wall stress increase with diameter (as it certainly does when employing idealised geometries) but also that the presence of ILT may significantly reduce wall stress, by up to 30% in their study. The inclusion of ILT into numerical analyses is routine nowadays as it is generally accepted that it does influence wall stress and is certainly important. On the other hand, however, some clinical studies [47, 56] have indicated that the ILT may not be as protective as generally believed.

One of the first reports to couple FE analyses together with patient-specific AAA 3D reconstructions was performed by Raghavan et al. [43] where, six AAA cases and one healthy control were examined, with very positive results. Fillinger et al. [18, 19] then furthered this work to show that peak wall stress may be superior to diameter in assessing rupture risk of patient-specific AAAs. These studies used large cohorts ($n = 48$ and $n = 103$, respectively) to determine statistical significance of results and concluded that not only is peak wall stress significantly higher in those cases that ruptured [18], but that peak wall stress seems superior to diameter in differentiating patients under observation who will experience catastrophic outcome [19]. Venkatasubramaniam et al. [60] concluded similar results in a smaller study group ($n = 27$). Peak wall stress appears to be an effective method of differentiating small AAAs that may be at risk of rupture also. Truijers et al. [54] reported that in a cohort of thirty small AAAs (diameter < 55 mm) that peak wall stress was significantly higher in ruptured cases compared to the repaired group.

Peak wall stress in the cohort examined for this chapter, showed that peak wall stress was on average ($\pm$ standard deviation) 56% significantly higher in the ruptured cases compared to the repaired group (0.89 ± 0.35 vs. 0.57 ± 0.23 MPa, $P = 0.018$), as shown in Fig. 3.

Peak wall stress appears to be repeatedly higher in ruptured AAAs compared to similarly-sized repaired AAAs and may be a very useful tool in helping with the decision-making process. However, to comprehensively determine the risk of rupture, one must account for the strength of the AAA wall also. Areas of high wall stress may be relatively safe from rupture due to the strength of the wall at that location, with wall strength known to vary significantly from region to region [44, 52]. Therefore, biomechanics-based rupture parameters have also been suggested, that may be even more superior than peak wall stress alone.

4.2 FEARI

The FEARI uses a ratio of wall stress to strength to assess the rupture threat. Wall stress can be easily estimated using the FEM, however, in vivo wall strength is

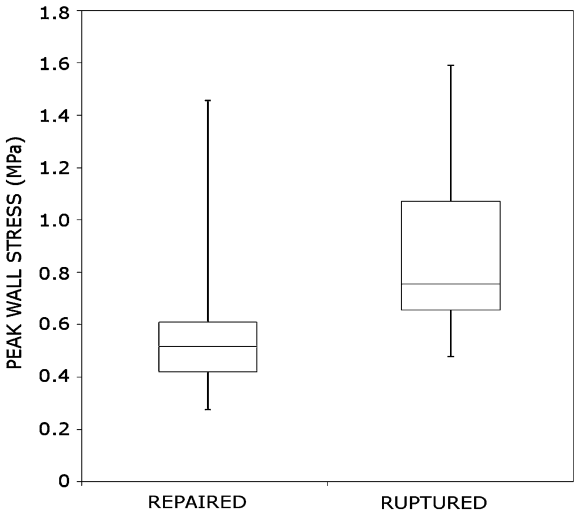

Fig. 3 Box and whisker plot of the peak wall stress results for the electively-repaired and ruptured cohort. The box plot represents the median, 25th and 75th percentiles with the whiskers representing the maximum and minimum values observed

significantly more difficult to obtain. There have been several reports published whereby the mechanical behaviour of AAA tissue has been presented [6, 42, 44, 52, 59]. By compiling the results from three large studies [42, 44, 52] and further analysing the location-dependent ultimate tensile strength (UTS), strength values based on a cohort of 69 patients and 149 tissue samples could be developed for each of the key regions. This wall strength is then used in conjunction with the peak wall stress measurement to assess the likelihood of rupture.

The FEARI method [10, 13] was applied to the study group of this chapter. 3D reconstructions were performed as before and wall stress computations determined using ABAQUS v6.9. All models were constrained proximally and distally to represent tethering to the remainder of the aorta, and a static uniform pressure loading of 120 mmHg was applied to the luminal surface. This standardised internal blood pressure allows the effect of geometry to be examined, as the variability of patient-specific blood pressure would add another uncertainty to the model. All models included the ILT and a uniform wall thickness of 1.5 mm. Fig. 4 illustrates the methodology behind the FEARI. Once the location of peak wall stress is determined, the stress is related to wall strength at that location. FEARI provides a rupture risk based on the ratio of stress to strength, with values larger than 1 indicating failure.

The results of the FEARI assessment (Fig. 5) indicate that the ruptured AAA cohort had a higher mean FEARI than the repaired group (1.03 ± 0.42 vs. 0.65 ± 0.3, $P = 0.019$). Maximum diameters were also 26% higher in the ruptured group (81.7 ± 12.5 vs. 64.7 ± 12.3 mm, $P = 0.0003$). The relationships between FEARI and maximum diameter in both the repaired and ruptured cohorts are insignificant (repaired, $P = 0.072$ and ruptured, $P = 0.174$). FEARI is possible through the mechanical testing of excised tissue in order to average population-mean UTS values for each of the primary locations in the AAA. The work to

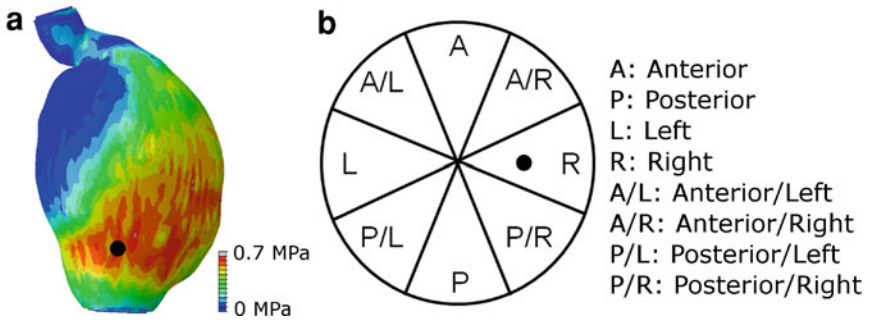

Fig. 4 FEARI methodology. **a** Peak wall stress quantity and location is determined using the FEM. **b** The location of peak wall stress corresponds to a distinct region, which in turn is assigned a wall strength value. FEARI then divides the peak wall strength by the wall strength at the location of peak stress to return a rupture index

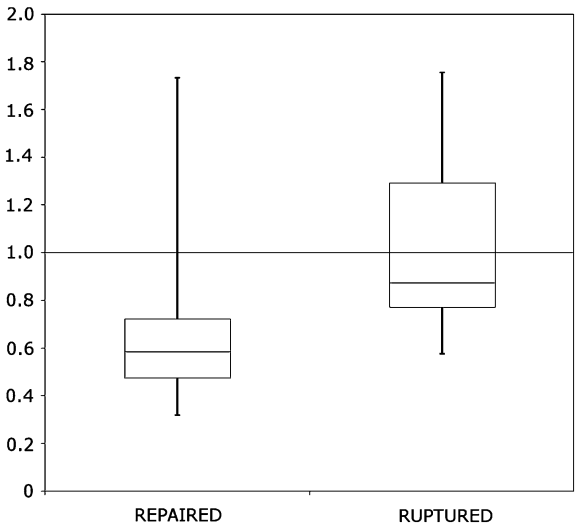

Fig. 5 FEARI results for the repaired and ruptured groups. The box plot represents the median, 25th and 75th percentiles with the whiskers representing the maximum and minimum values observed

date using the FEARI model is based on the previous tests of others and therefore the approach can be improved. A large multi-centre study involved in the excision and testing of tissue would help strengthen the FEARI wall strength data, thus strengthening the applicability of the tool.

It is also possible to statistically estimate patient-specific wall strength thanks to the work of Vande Geest et al. [58]. This approach allows a point-wise wall strength estimation which can be coupled with the point-wise wall stress estimations from numerical analyses to create the RPI as discussed in Chap. 3.

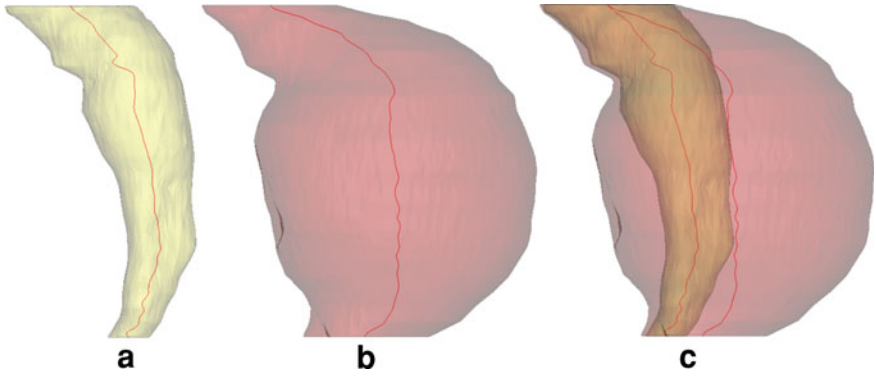

Fig. 6 Comparison of the centrelines generated from the lumen geometry (**a**) and the complete AAA volume, including ILT (**b**), and the visual difference in both centrelines (**c**)

4.3 Asymmetry

In 2009, a method of measuring asymmetry in the anterior-posterior plane of AAAs was reported [9] with this asymmetry correlated to both peak and posterior wall stress. This previous publication had some significant limitations, however, and work has continued since to address these shortcomings. Firstly, anterior-posterior asymmetry is essentially 2D and although the majority of AAAs naturally bulge outward in this direction due to the constraint of the spine, this measurement excludes certain AAAs. A new method of measurement has been recently developed by the authors whereby the asymmetry is measured in 3D therefore, all AAAs can be investigated. Another major limitation of this earlier report was the omission of the ILT. For any meaningful numerical analyses, ILT must be incorporated into the model. In the latest work, the ILT is modeled using the material model of Wang et al. [64] as mentioned previously. Within the finite element analysis, the use of shell elements have been replaced with 3D solid stress elements which are deemed a more accurate modeling approach compared to shell elements [7, 34], in particular when analysing these complex 3D simulations.

Therefore, for this aspect of the CADq, the 3D asymmetry of the study group used throughout this chapter was measured. When determining the asymmetry for AAA models in the presence of ILT, two centrelines are generated, one for the lumen and one for the luminal surface of AAA wall (Fig. 6). The method of measurement of 3D asymmetry remains similar to that of 2D asymmetry, in that the centreline is connected with an axis and the asymmetry defined as the distance from this axis to the centreline. However, as AAA centrelines are tortuous and travel through three dimensions, the distance from the centreline is now measured in three dimensions also. This updated measurement technique can be seen in Fig. 7. A further refinement to the tool can be made by smoothing the centrelines generated within the reconstruction software, as slight changes in geometry can result in large changes in the centreline.

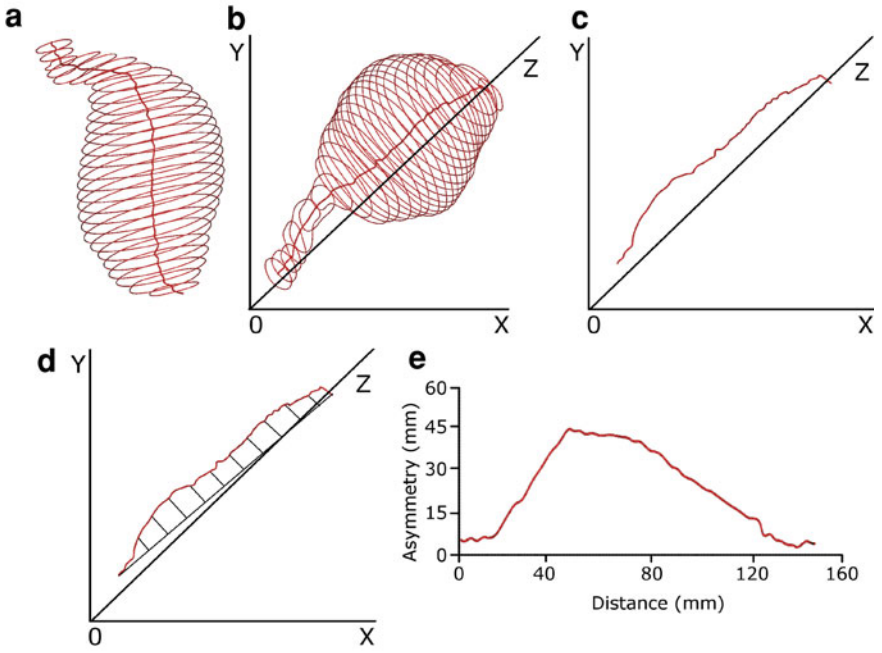

Fig. 7 Process of determining 3D asymmetry. **a** Polylines and centrelines are generated from the 3D reconstruction and **b** then plotted in 3D using our custom-built program. The program then automatically **c** isolates the centreline and **d** connects the ends of the centreline. The distance from this connecting axis to the centreline is then measured through three dimensions before **e** the program then automatically graphs the asymmetry along the length of the AAA

The CADq asymmetry results (Fig. 8) observed in this study show that the mean lumen asymmetry is 33% higher for the ruptured group, yet the difference was not significant ($P = 0.1$). The AAA wall asymmetry was only 3% higher in the ruptured group. By correlating the maximum wall stress to both the maximum diameter and the lumen asymmetry, it was noted that the lumen asymmetry is more significantly correlated to maximum wall stress for the repaired ($P = 0.002$) and ruptured ($P = 0.033$) groups compared to diameter for the same groups (repaired, $P = 0.032$; ruptured, $P = 0.174$).

Asymmetry as a CADq tool can be used as an additional technique to identify high-risk AAAs where diameter may fail. By comparing similarly-sized AAAs from the repaired and ruptured groups, it was seen that asymmetry may be useful alongside diameter. The AAAs compared in Fig. 9a were both large 11 cm AAAs, where one had ruptured and one was electively-repaired. The diameters of both AAAs were comparable but the resulting peak wall stress of the ruptured aneurysm was 157% higher than the repaired case (1.13 vs. 0.44 MPa) and the maximum measured lumen asymmetry was 125% higher in the ruptured AAA (45 vs.

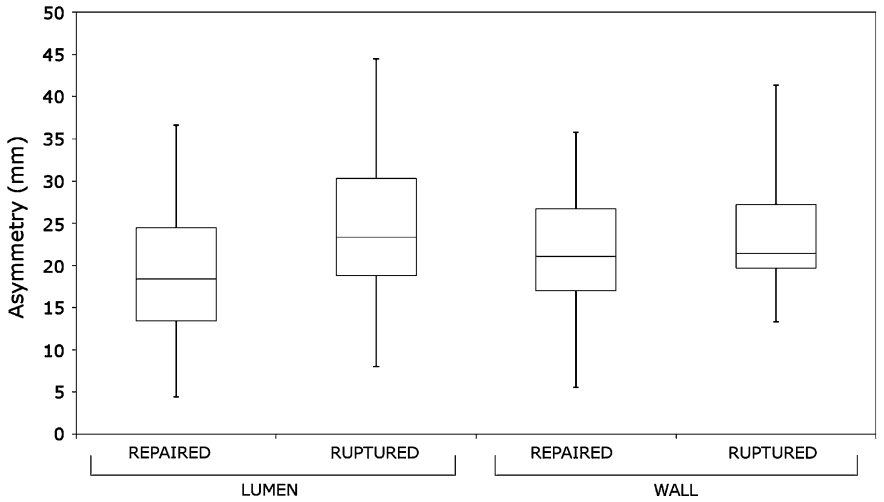

Fig. 8 Asymmetry results for both the lumen centrelines and the AAA wall centrelines for the repaired and ruptured groups. The box plot represents the median, 25th and 75th percentiles with the whiskers representing the maximum and minimum values observed

20 mm). The use of asymmetry also applies in some smaller AAAs. In the two aneurysms shown in Fig. 9b, both of which are 6.5 cm in maximum transverse diameter, the results show that the peak wall stress is 184% higher in the ruptured case (1.39 vs. 0.49 MPa) and the maximum lumen asymmetry is 157% higher in the ruptured case (18 vs. 7 mm). However, care should be taken when interpreting these preliminary results. The results presented in Fig. 8 show there can be a large distribution in asymmetry results and the measurement is not necessarily higher in ruptured cases. Increasing the numbers of cases examined may help reduce the distribution of results as there are only 10 patients in the ruptured cohort and only 42 in the repaired group.

5 Validation of CAD

Validation of numerical tools in the context of AAA rupture-prediction is difficult to achieve [33], with the benefits and challenges of patient-specific risk assessment well documented [2]. In vitro validation of numerical modeling was recently performed [14] where patient-specific silicone rubber AAA models were manufactured and then ruptured. High-speed photography was used to capture the event of rupture, with FEA used to validate the rupture locations. Excellent agreement in the experimental and computational results was observed with FEA accurately predicting the location of rupture in 90% of the models examined. The 10% that did not correlate were found to contain flaws within the wall as a result of the

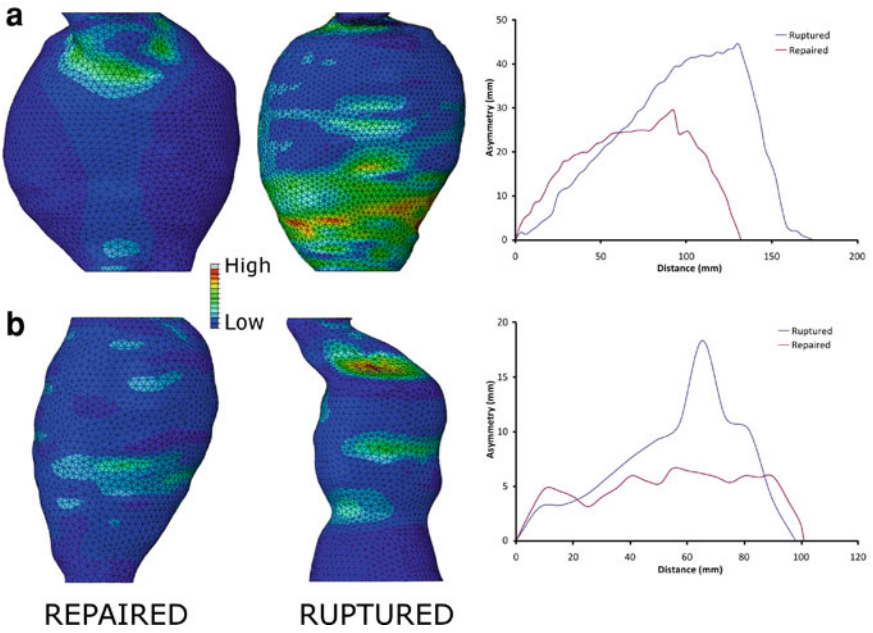

Fig. 9 **a** Comparison of an 11 cm repaired AAA and an 11 cm ruptured case. Measured lumen asymmetry for both cases is presented on the right. Both peak wall stress (1.13 vs. 0.44 MPa) and lumen asymmetry (45 vs. 20 mm) were higher in the ruptured case, whereas diameter did not differentiate. **b** Comparison of a 6.5 cm repaired AAA and a 6.5 cm ruptured case. Measured lumen asymmetry for both cases is presented on the right. Both peak wall stress (1.39 vs. 0.49 MPa) and lumen asymmetry (18 vs. 7 mm) were again higher in the ruptured case, with diameter identifying them both as high-risk (diameters >5.5 cm). Models are not shown to scale

manufacturing process, thus altering the burst site. In vivo validation however, is significantly more challenging.

However, recently a 73 year old male presented himself to a local vascular outpatients department with intermittent claudication. The clinician examined the patient with ultrasound and observed a 7.5 cm AAA (Fig. 10a). CT imaging was subsequently performed (Fig. 10b) and endovascular aneurysm repair (EVAR) planned. Exactly one week after CT imaging, the patient collapsed at a pre-operative assessment clinic complaining of acute abdominal pain and nausea. The patient was transferred to the HSE Midwestern Regional Hospital, Limerick and was hypotensive (80/40 mmHg) on arrival. The clinicians immediately performed a laparotomy and open surgical repair of the leaking infrarenal AAA. During the procedure the clinicians sketched (Fig. 11a) and later recorded the location of rupture on the CT image (Fig. 11b). The patient fully recovered from the operation and was discharged nine days later with no complications.

The CT dataset of this case was imported into Mimics and analysed by the author using the techniques outlined throughout this chapter. The model was

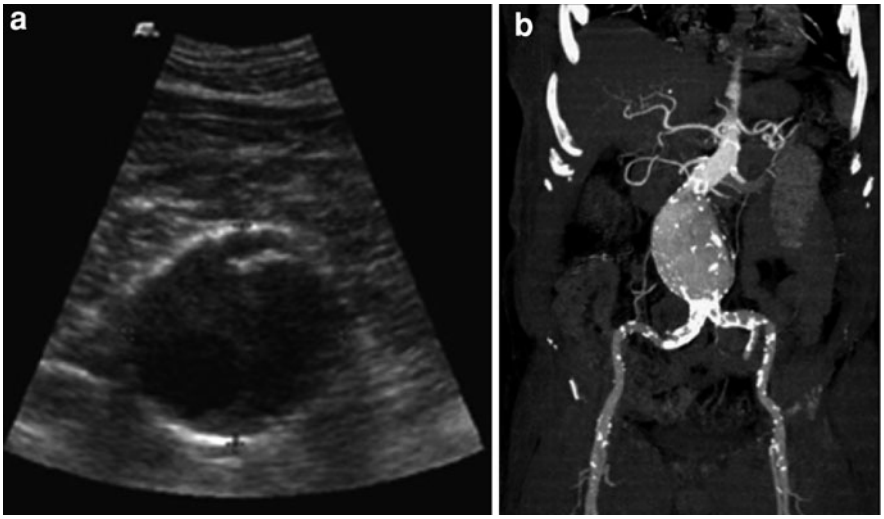

Fig. 10 **a** Ultrasound image showing the patient's 7.5 cm AAA and **b** CT image showing the infrarenal AAA from the anterior view

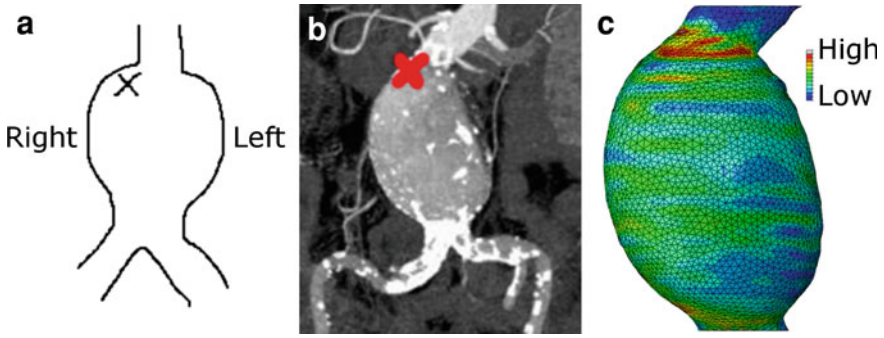

Fig. 11 Comparison of clinical rupture locations with the FEA-predicted location of peak wall stress. **a** Intraoperative sketch of AAA rupture site. **b** Clinicians then recorded the rupture site on the CT image. **c** Resulting FEA-predicted wall stress distribution (Peak wall stress = 0.719 MPa)

examined with finite element analysis using a uniform wall thickness of 1.5 mm and the standard AAA wall [41] and ILT [64] material properties. The exact location of rupture was withheld from the author to ensure there was no bias in the modeling approach. Wall stress results (Fig. 11c) showed that the AAA experienced high wall stress ($\sim$0.7 MPa) located at the anterior-right proximal inflection region of the AAA sac. An excellent correlation was observed when the location of FEA-predicted peak stress was compared with the actual rupture site (Fig. 11). According to our FEARI model this particular case presented an 85%

chance of rupture (FEARI = 0.85) based on a peak wall stress of 0.719 MPa located at the anterior-right region (wall strength = 0.847 MPa).

6 Conclusion

Numerical modeling of AAAs is becoming more prevalent with several laboratories working towards improving AAA risk-prediction. To date, these efforts remain essentially un-validated and the brief description of the validation procedure presented here is one of the few reports of correlation between numerical and clinical rupture sites [54]. However, regardless of the efforts underway and the regular improvements in numerical modeling, possibly the biggest barrier to CAD becoming a clinical tool is the difficulty in translating the approach to the clinic. Neal and Kerckhoffs [39] recently reported on the current progress of patient-specific modeling, concluding that the incorporation of patient-specific modeling into the workflow of the clinician will require, among other things, regulatory approval by the relevant bodies, for example, the Food and Drug Administration (FDA). The techniques presented in this chapter are relatively easy to translate to the clinic as results of peak wall stress, FEARI and asymmetry can be obtained within approximately 3 h of CT imaging and therefore these tools would not detract from the treatment course of the patient. Wall stress has been repeatedly shown to be higher in symptomatic/ruptured AAAs compared to electively-repaired cases [13, 18–20, 30, 54, 60] and the results reported here agree with these previous studies. However, further refinement of CAD, in particular CADe of the AAA wall is vital if patient-specific analysis is desired. The aortic wall thickness remains elusive from current CT and MR imaging. A method of detecting the wall thickness was reported by Martufi et al. [32] however the technique is yet to be fully adopted within the numerical models of others. Assuming a uniform wall thickness in numerical models may be a gross assumption as it is known that the wall thickness influences the wall stress [48, 53, 60], yet in the CAD validation presented in Sect. 5 and in the work of Truijers et al. [54], a uniform wall thickness was employed and the location of rupture was still predicted. A similar finding was observed in studies on an idealised AAA model [12] where the wall thickness was varied according to the measured wall thickness in a silicone idealised AAA analogue. Although wall thickness does alter the numerical quantities of wall stress, it may not significantly influence the stress patterns to the same extent. In this previous report the overall trend in wall stress distribution remained similar regardless of wall thickness, that is, wall stress was higher at the proximal and distal inflection regions than that found in the area of maximum diameter.

It is understood that it may be unlikely these tools will ever directly replace the use of maximum diameter as clinicians will always feel that large AAAs represent a rupture-threat and should be repaired. It is the small to

medium-sized AAAs however, that could be examined using these alternative diagnostic tools, and someday may prove to be a useful adjunct to maximum diameter.

References

1. Bluestein, D., Dumont, K., De Beule, M., Ricotta, J., Impellizzeri, P., Verhegghe, B., Verdonck, P.: Intraluminal thrombus and risk of rupture in patient-specific abdominal aortic —FSI modeling. Comput. Methods Biomech Biomed Eng. **12**, 73–81 (2009)
2. Breeuwer, M., de Putter, S., Kose, U., Speelman, L., Visser, K., Gerritsen, F., Hoogeveen, R., Krams, R., van den Bosch, H., Buth, J., Gunther, T., Wolters, B., van Dam, E., van de Vosse, F.: Towards patient-specific risk assessment of abdominal aortic aneurysm. Med. Biol. Eng. Comput. **46**, 1085–1095 (2008)
3. Conway, K.P, Byrne, J., Townsend, M., Lane, IF.: Prognosis of patients turned down for conventional abdominal aortic aneurysm repair in the endovascular and sonographic era: Szilagyi revisted? J. Vasc. Surg. **33**, 752–757 (2001)
4. Cronenwett, J.L., Murphy, T.F., Zelenock, G.B., Whitehouse, Jr W.M., Lindenauer S.M., Graham, L.M., Quint, L.E., Silver T.M., Stanley, J.C.: Actuarial analysis of variables associated with rupture of small abdominal aortic aneurysms. Surgery **98**, 472–483 (1985)
5. Darling, R.C., Messina, C.R., Brewster D.C., Ottinger L.W.: Autopsy study of unoperated abdominal aortic aneurysms. The case for early resection. Circulation **56**, 161–164 (1977)
6. Di Martino, E.S., Bohra, A., Vande Geest, J.P., Gupta, N., Makaroun M.S., Vorp, D.A.: Biomechanical properties of ruptured versus electively repaired abdominal aortic aneurysm wall tissue. J. Vasc. Surg. **43**, 570–576 (2006)
7. Doyle, B.J., Callanan, A., McGloughlin, T.M.: A comparison of modelling techniques for computing wall stress in abdominal aortic aneurysms. Biomed. Eng. Online **6**, 38 (2007)
8. Doyle, B.J., Morris, L.G., Callanan, A., Kelly, P., Vorp, D.A., McGloughlin, T.M.: 3D reconstruction and manufacture of real abdominal aortic aneurysms: From CT scan to silicone model. J. Biomech. Eng. **130**, 034501 (2008)
9. Doyle, B.J., Callanan, A., Burke, P.E., Grace, P.A., Walsh, M.T., Vorp, D.A., McGloughlin, T.M.: Vessel asymmetry as an additional tool in the assessment of abdominal aortic aneurysms. J. Vasc. Surg. **49**, 443–454 (2009)
10. Doyle, B.J., Callanan, A., Walsh M.T., Grace P.A., McGloughlin, T.M.: A finite element analysis rupture index (FEARI) as an additional tool for abdominal aortic aneurysm rupture prediction. Vasc. Dis. Prev. **6**, 114–121 (2009)
11. Doyle, B.J., Grace, P.A., Kavanagh, E.G., Burke, P.E., Wallis, F., Walsh, M.T., McGloughlin, T.M.: Improved assessment and treatment of abdominal aortic aneurysms: The use of 3D reconstructions as a surgical guidance tool in endovascular repair. Ir. J. Med. Sci. **178**, 321–328 (2009)
12. Doyle, B.J., Corbett, T.J., Callanan, A., Walsh, M.T., Vorp, D.A., McGloughlin, T.M.: An experimental and numerical comparison of the rupture locations of an abdominal aortic aneurysm. J. Endovasc. Ther. **16**, 322–335 (2009)
13. Doyle, B.J., Coyle, P., Kavanagh, E.G., Grace, P.A., McGloughlin, T.M.: A finite element analysis rupture index (FEARI) assessment of electively repaired and symptomatic/ruptured abdominal aortic aneurysms. IFMBE Proc. **31**, 883–886 (2010)
14. Doyle, B.J., Cloonan, A.J., Walsh, M.T., Vorp, D.A., McGloughlin, T.M.: Identification of rupture locations in patient-specific abdominal aortic aneurysms using experimental and computational techniques. J. Biomech. **43**, 1408–1416 (2010)
15. Elger, D.F., Blackletter, D.M., Budwig, R.S., Johansen, K.H.: The influence of shape on the stresses in model abdominal aortic aneurysms. J. Biomech. Eng. **118**, 326–332 (1996)

16. Ernst, C.B.: Abdominal aortic aneurysm. N. Eng. J. Med. **328**, 1167–1172 (1993)
17. Fenton, J.J., Taplin, S.H., Carney, P.A., Abraham, L., Sickles, E.A., D'Orsi, C., Berns, E.A., Cutter, G., Hendrick, E., Barlow, W.E., Elmore, J.G.: Influence of computer-aided detection on performance of screening mammography. N. Eng. J. Med. **356**, 1399–1409 (2007)
18. Fillinger, M.F., Raghavan, M.L., Marra, S.P., Cronenwett, J.L., Kennedy F.E.: In vivo analysis of mechanical wall stress and abdominal aortic aneurysm rupture risk. J. Vasc. Surg. **36**, 589–597 (2002)
19. Fillinger, M.F., Marra, S.P., Raghavan, M.L., Kennedy, F.E.: Prediction of rupture risk in abdominal aortic aneurysm during observation: wall stress versus diameter. J. Vasc. Surg. **37**, 724–732 (2003)
20. Gasser, T.C., Auer, M., Labruto, F., Swedenborg, J., Roy, J.: Biomechanical rupture risk assessment of abdominal aortic aneurysms: model complexity versus predictability of finite element simulations. Eur. J. Vasc. Endovasc. Surg. (2010). doi:10.1016/j.ejvs.2010.04.003
21. Giannoglu, G., Giannakoulas, G., Soulis, J., Chatzizisis, Y., Perdikides, T., Melas, N., Parcharidis, G., Louridas, G.: Predicting the risk of rupture of abdominal aortic aneurysms by utilizing various geometrical parameters: revisiting the diameter criterion. Angiology **57**, 487–494 (2006)
22. Glimaker, H., Holmberg, L., Elvin, A., Nybacka, O., Almgren. B., Bjorck, C.G., Eriksson, I.: Natural history of patients with abdominal aortic aneurysm. Eur. J. Vasc. Surg. **5**, 125–130 (1991)
23. Hirose, Y., Takamiya, M.: Growth curve of ruptured aortic aneurysm. J. Cardiovasc. Surg. **39**, 9–13 (1998)
24. Inzoli, F., Boschetti, F., Zappa, M., Longo, T., Fumero, R.: Biomechanical factors in abdominal aortic aneurysm rupture. Eur. J. Vasc. Surg. 7, 667–674 (1993)
25. Kleinstreuer, C., Li, Z.: Analysis and computer program for rupture risk prediction of abdominal aortic aneurysms. Biomed. Eng. Online **5**, 19 (2006)
26. Lederle, F.A., Johnson, G.R., Wilson, S.E., Ballard, D.J., Jordan Jr ,W.D., Blebea, J., Littooy, F.N., Freischlag, J.A., Bandyk, D., Rapp, J.H., Salam, A.A.: Rupture rate of large abdominal aortic aneurysms in patients refusing or unfit for elective repair. JAMA **287**, 2968–2972 (2002)
27. Leung, J.H., Wright, A.R., Cheshire, N., Crane, J., Thom, S.A., Hughes, A.D., Xu Y Fluid structure interaction of patient specific abdominal aortic aneurysms: a comparison with solid stress models. Biomed. Eng. Online **5**, 33 (2006)
28. Li, Z.Y., U-King-Im, J., Tang, T.Y., Soh, E., See, T.C., Gillard, J.H.: Impact of calcification and intraluminal thrombus on the computed wall stresses of abdominal aortic aneurysm. J. Vasc. Surg. **47**, 928–935 (2008)
29. Lorensen, W.E., Cline, H.E.: Marching cubes: a high resolution 3D surface construction algorithm. Comp. Graphics **21**, 163–169 (1987)
30. Maier, A., Gee, M.W., Reeps, C., Pongratz, J., Eckstein, H.H., Wall, W.A.: A comparison of diameter, wall stress, and rupture potential index for abdominal aortic aneurysm rupture risk prediction. Ann. Biomed. Eng. **38**, 3124–3134 (2010)
31. Maier, A., Gee, M.W., Reeps, C., Eckstein, H.H., Wall, W.A.: Impact of calcifications on patient-specific wall stress analysis of abdominal aortic aneurysms. Biomech. Model. Mechanobiol. **9**, 511–521 (2010)
32. Martufi, G., DiMartino, E.S., Amon, C.H., Muluk, S.C., Finol, E.A.: Three-dimensional geometrical characterization of abdominal aortic aneurysms: image-based wall thickness distribution. J. Biomech. Eng. **131**, 061015 (2009)
33. McGloughlin, T.M., Doyle, B.J.: New approaches to abdominal aortic aneurysm rupture risk assessment: engineering insights with clinical gain. Arterioscler. Thromb. Vasc. Biol. **30**, 1687–1694 (2010)
34. Meyer, C.A., Guivier-Curien, C., Moore, J.E.: Trans-thrombus blood pressure effects in abdominal aortic aneurysms. J. Biomech. Eng. **132**, 071005 (2010)

35. Moore, J.A., Steinman, D.A., Ethier, C.R.: Computational blood flow modeling: errors associated with reconstructing finite element models from magnetic resonance images. J. Biomech. **31**, 179–184 (1998)
36. Morris, L., Delassus, P., Callanan, A., Walsh, M., Wallis, F., Grace, P., McGloughlin, T.: 3D numerical simulation of blood flow through models of the human aorta. J. Biomech. Eng. **127**, 767–775 (2005)
37. Mower, W.R., Baraff, L.J., Sneyd, J.: Stress distributions in vascular aneurysms: factors affecting risk of aneurysm rupture. J. Surg. Res. **55**, 155–161 (1993)
38. National Health Service. National Screening Program for Abdominal Aortic Aneurysm [online] available: http://aaa.screening.nhs.uk (2009). Accessed 9 Feb 2009
39. Neal, M.L., Kerckhoffs, R.: Current progress in patient-specific modeling. Brief Bioinform. **11**, 111–126 (2009)
40. Nicholls, S.C., Gardner, J.B., Meissner, M.H., Johansen, H.K: Rupture in small abdominal aortic aneurysms. J. Vasc. Surg. **28**, 884–888 (1998)
41. Raghavan, M.L., Vorp, D.A.: Toward a biomechanical tool to evaluate rupture potential of abdominal aortic aneurysm: identification of a finite strain constitutive model and evaluation of its applicability. J. Vasc. Surg. **33**, 475–482 (2000)
42. Raghavan, M.L., Webster, M.W., Vorp, D.A.: Ex vivo biomechanical behaviour of abdominal aortic aneurysm: assessment using a new mathematical model. Ann. Biomed. Eng. **24**, 573–582 (1996)
43. Raghavan, M.L., Vorp, D.A., Federle, M.P., Makaroun, M.S., Webster, M.W.: Wall stress distribution on three-dimensionally reconstructed models of human abdominal aortic aneurysm. J. Vasc. Surg. **31**, 760–769 (2000)
44. Raghavan, M.L., Kratzberg, J., de Tolosa, E.M.C., Hanaoka, M.M., Walter, P., da Silva, E.S.: Regional distribution of wall thickness and failure properties of human abdominal aortic aneurysm. J. Biomech. **39**, 3010–3016 (2006)
45. Sacks, M.S, Vorp, D.A, Raghavan, M.L., Federle, M.P, Webster, M.W.: In vivo three-dimensional surface geometry of abdominal aortic aneurysms. Ann. Biomed. Eng. **27**, 469–479 (1999)
46. Sayers, R.D.: Aortic aneurysms, inflammatory pathways and nitric oxide. Ann. Royal Col. Surg. Eng. **84**, 239–246 (2002)
47. Schurink, G.W.H., van Baalen, J.M., Visser, M.J.T., van Bockel, J.H.: Thrombus within an aortic aneurysm does not reduce pressure on the aneurysmal wall. J. Vasc. Surg. **31**, 501–506 (2000)
48. Scotti, C.M., Shkolnik, A.D., Muluk, S.C., Finol, E.: Fluid-structure interaction in abdominal aortic aneurysms: effect of asymmetry and wall thickness. Biomed. Eng. Online **4**, 64 (2005)
49. Speelman, L., Bohra, A, Bosboom, E.M.H., Schurink, G.W.H., van de Vosse, F.N., Makaroun, M.S., Vorp, D.A.: Effects of wall calcifications in patient-specific wall stress analyses of abdominal aortic aneurysms. J. Biomech. Eng. **129**, 1–5 (2007)
50. Stenbaek, J., Kalin, B., Swedenborg, J.: Growth of thrombus may be a better predictor of rupture than diameter in patients with abdominal aortic aneurysms. Eur J Vasc Endovasc Surg **20**, 466–469 (2000)
51. Stringfellow, M.M., Lawrence, P.F., Stringfellow, R.G.: The influence of aorta geometry upon stress in the aneurysm wall. J. Surg. Res. **42**, 425–433 (1987)
52. Thubrikar, M.J., Labrosse, M., Robicsek, F., Al-Soudi, J., Fowler, B.: Mechanical properties of abdominal aortic aneurysm wall. J. Med. Eng. Tech. 25:133–142 (2001)
53. Thubrikar M.J, Al-Soudi, J., Robicsek, F.: Wall stress studies of abdominal aortic aneurysm in a clinical model. Ann. Vasc. Surg. **15**, 355–366 (2001)
54. Truijers M., Pol, J.A., SchultzeKool, L.J., van Sterkenburg, S.M., Fillinger, M.F., Blankensteijn, J.D.: Wall stress analysis in small asymptomatic, symptomatic and ruptured abdominal aortic aneurysms. Eur. J. Vasc. Endovasc. Surg. **33**, 401–407 (2007)
55. United States Preventative Services Task Force. Screening for abdominal aortic aneurysm: recommendation statement. Ann. Int. Med. **142**, 198–202 (2005)

56. Vallabhaneni, S.R., Gilling-Smith, G.L., Brennan, J.A., Heyes, R.R., Hunt, J.A., How, T.V., Harris, P.L.: Can intrasac pressure monitoring reliably predict failure of endovascular aneurysm repair? J. Endovasc. Ther. **10**, 524–530 (2003)
57. Vande Geest, J.P., Di Martino, E.S., Bohra, A., Makaroun, M.S., Vorp, D.A.: A biomechanics-based rupture potential index for abdominal aortic aneurysm risk assessment. Ann. NY Acad. Sci. **1085**, 11–21 (2006)
58. Vande Geest, J.P., Wang, D.H.J., Wisniewski, S.R., Makaroun, M.S., Vorp, D.A.: Towards a non-invasive method for determination of patient-specific wall strength distribution in abdominal aortic aneurysms. Ann. Biomed. Eng. **34**, 1098–1106 (2006)
59. Vande Geest, J.P., Sacks, M.S, Vorp, D.A.: The effects of aneurysm on the biaxial mechanical behaviour of human abdominal aorta. J. Biomech. **39**, 1324–1334 (2006)
60. Venkatasubramaniam, A.K., Fagan, M.J., Mehta, T., Mylankal K.J., Ray, B., Kuhan, G., Chetter, I.C., McCollum, P.T.: A comparative study of aortic wall stress using finite element analysis for ruptured and non-ruptured abdominal aortic aneurysms. Eur. J. Vasc. Endovasc. Surg. **28**, 168–176 (2004)
61. Volokh, K.Y., Vorp, D.A.: A model of growth and rupture of abdominal aortic aneurysm. J. Biomech. **41**, 1015–1021 (2008)
62. Vorp, DA.: Biomechanics of abdominal aortic aneurysm. J. Biomech. **40**, 1887–1902 (2008)
63. Vorp, D.A., Raghavan, M.L., Webster, M.W.: Mechanical wall stress in abdominal aortic aneurysm: influence of diameter and asymmetry. J. Vasc. Surg. **27**, 632–639 (1998)
64. Wang, D.H.J., Makaroun, M.S., Webster, M.W., Vorp, D.A.: Mechanical properties and microstructure of intraluminal thrombus from abdominal aortic aneurysm. J. Biomech. Eng. **123**, 536–539 (2001)
65. Wang, D.H.J., Makaroun, M.S., Webster, M.W., Vorp, D.A.: Effect of intraluminal thrombus on wall stress in patient-specific models of abdominal aortic aneurysm. J. Vasc. Surg. **36**, 598–604 (2002)
66. Watton, P., Hill, N., Heil, M.: A mathematical model for the growth of the abdominal aortic aneurysm. Biomech. Model. Mechanobiol. **3**(2), 98–113 (2004)
67. Wilarusmee, C., Suvikrom, J., Suthakorn, J., Lertsithichai, P., Sitthiseriprapip, K., Proprom, N., Kittur, D.S.: Three-dimensional aortic aneurysm model and endovascular repair: an educational tool for surgical trainees. Int. J. Angiol. **17**, 129–133 (2008)
68. Xiong, J., Wang, S.M., Zhou, W., Wu, J.G.: Measurement and analysis of ultimate mechanical properties, stress-strain curve fit, and elastic modulus formula of human abdominal aortic aneurysm and nonaneurysmal abdominal aorta. J. Vasc. Surg. **48**, 189–195 (2008)
69. Zienkiewicz, O.C., Taylor, R.L., Zhu, J.Z.: The finite element method: its basis and fundamentals, 6th edn. Elsevier Butterworth-Heinemann, UK (2005)